PERFORMANCE CHARACTERISTICS EVALUATION OF UNSTEADY PULSE JET EJECTOR-EXPERIMENTAL AND MODEL RESULTS

E. M. Marzouk, A. F. Abdel Wahab, M.A. Awwad and A.I. Abdelfattah

Mechanical Engineering Department, Faculty of Engineering
Alexandria University Alexandria 21544, Egypt

ABSTRACT

Pulsed ejectors are essential devices in pulsed pressure gain combustors for gas turbines, in the pulse converter turbocharging for I.C.E., ..etc. The development of these devices has proceeded by trial and intuition. A comprehensive experimental and theoretical investigation of unsteady pulse jet ejector is presented. The experimental performance characteristics compare favorably with model predictions. Particular emphasis is placed towards optimization of geometric and operational parameters on the augmenter to maximize ejector performance based on mass and thrust augmentation. The results show that the performance is dependent on both the primary flow configuration, which is responsible for the generation of strong pressure wave action in the augmenter and also on the augmenter tube itself to allow for the proper and tuned propagation of the generated pressure waves to augment the primary flow to maximum. The augmenter length to diameter ratio is shown to vary according to the primary flow frequency. An optimum augmenter to primary tubes area ratio of 4.15 is obtained for thrust augmentation.

Keywords Pulse ejector, Theoretical, Experimental, Optimization

INTRODUCTION

The pulsed ejector is used in for pumping and thrust augmentation applications. It employs the unsteady intermittent (pulsed) primary flow to generate repeated pressure exchange cycles in the augmenter tube in order to augment both the primary mass flow rate and thrust.

Pulsed ejector, presenting superior augmentation capacity than steady flow ejectors, have been thus employed in unsteady flow applications where thrust and mass augmentation represented crucial importance. One such application is the pulsed combustor systems for diverse applications [1-3]. The unsteady flow ejectors performance of both the inlet backflow and tail pipe outflow of a single aerovalve pulsed combustor. An early version (Figure 1-a [4]) and more recent configuration (Figure 1-b [5,6]), are of discrete importance for the aimed pressure gain potential to be realized across the complete pressure-gain pulsating combustor. Another application of the pulsed ejector is in the pulse converter turbocharging (see Figure 2) which is developed to maintain both the advantage of pulse tubocharging to convey exhaust energy to the turbine with minimum losses [7,8] and also at the same time have the advantage of constant pressure turbocharging with fully admitted flow through turbine of turbocharger despite the inherent unsteady nature of the exhaust flows [9].

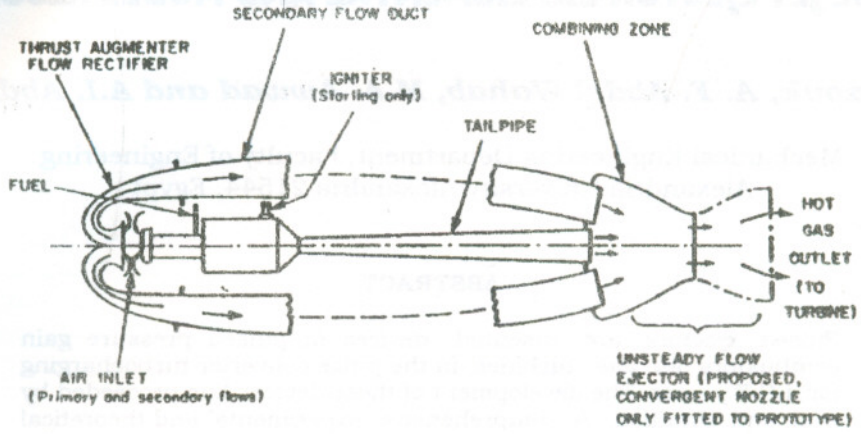

(a)

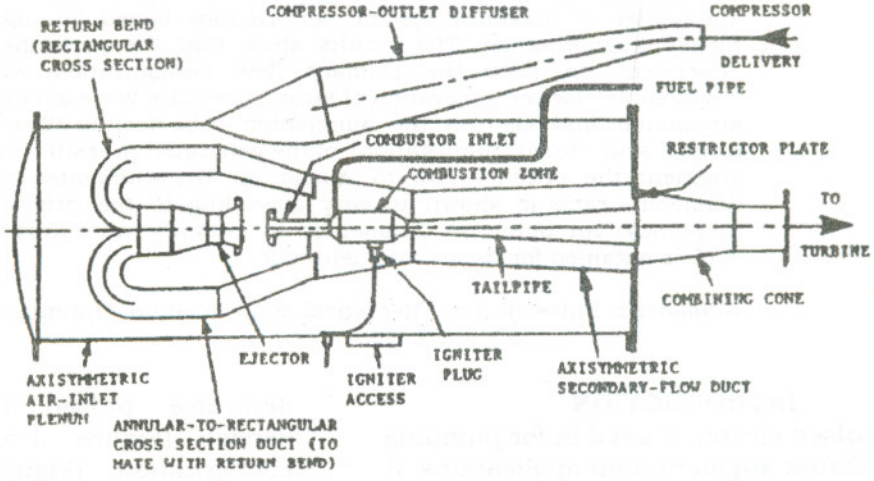

(b)

Figure 1 Diagrammatic configuration of pulsed, pressure-gain combustor; (a) Early version [4], (b) Recent version [6]

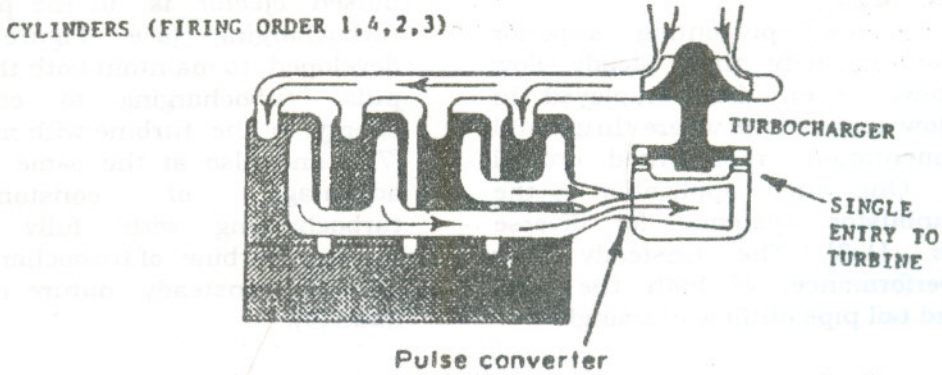

Figure 2 Pulse converter turbocharging as applied to four cylinder engine.

So far, the design and development of pulsed ejectors have proceeded largely by trial and intuition, a method that is time consuming, costly and does not guarantee an optimum design [3-5, 10, 11].

A model for the pulsed ejector is presented by Marzouk *et al.* [12]. The model is based on the modified method of characteristics for prediction on one-dimension, non-steady compressible flow with the influence to permit account for area change, friction and heat transfer. The numerical procedure is set up for computer coding with sufficient generality to include all significant processes which occur in the primary and augmenter tubes. Very good correlation and agreement is demonstrated between the experimental measurements and numerical results [12]. Therefore, it is concluded that the model is capable of interpreting the phenomena within the ejector with high accuracy.

The present work shows the performance characteristics of the pulse jet ejector under variation of the important geometric and operational parameters. Particular emphasis is placed on experimental measurements to validate performance behavior. In addition the model is used to explain many performance features of these pulsed ejectors.

Experimental Description

The pulse jet ejector is shown schematically in Figure 3. The experimental ejector is detailed in Figure 4. It comprises the pulsating flow generator that produces the intermittent flow in the primary tube. The primary tube exit port and augmenter inlet port are sealed within a plenum chamber from which secondary flow is drawn through the augmenter. The chamber is equipped with a BS standard flow nozzle for secondary flow measurement.

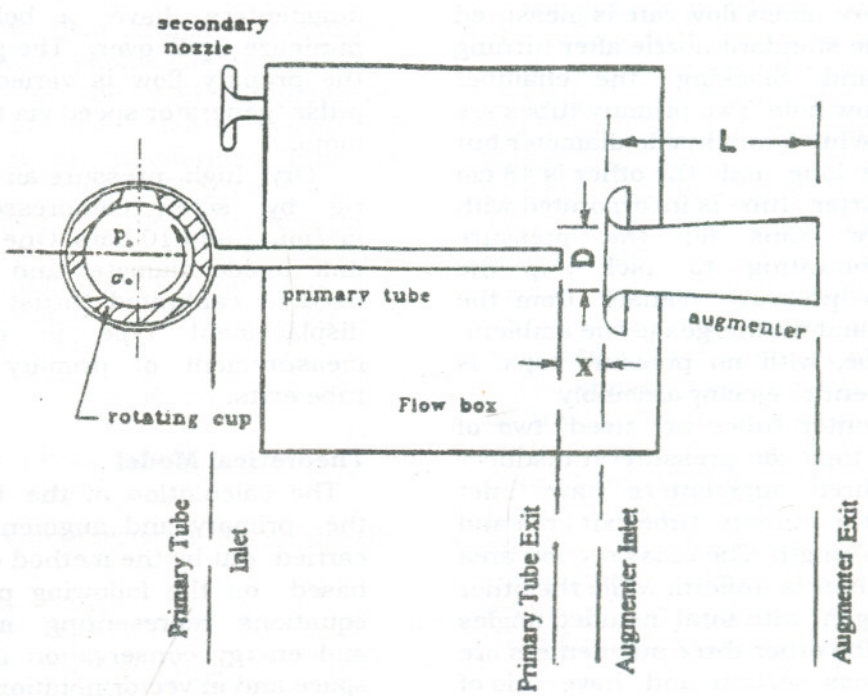

Figure 3 Schematic diagram of a prototype pulsed ejector.

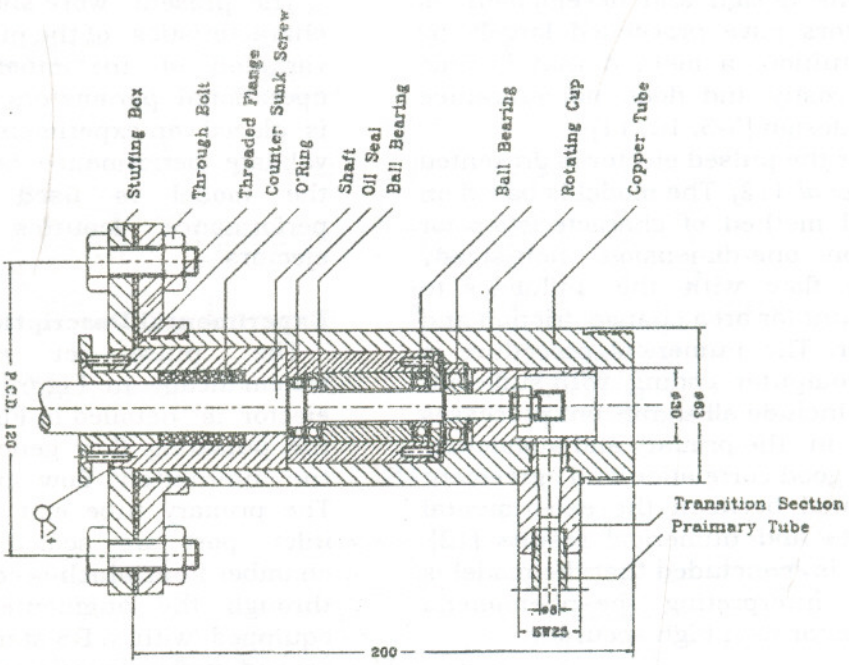

Figure 4 Constructional drawing of a pulse generator.

The primary mass flow rate is measured using the same standard nozzle after turning it around and blocking the chamber augmenter flow hole. Two primary tubes are used, each having 8 mm inside diameter but one is 40 cm long and the other is 48 cm long. The shorter tube is incorporated with two pressure taps for the pressure transducer mounting to pick up the instantaneous pressure signals from the primary flow and discharges to the ambient. The other tube, with no pressure taps, is used with the entire ejector assembly.

Six augmenter tubes are used, two of which have taps for pressure transducer mounting. Three augmenters have inlet areas 4 times the primary tube exit area and are 24 cms in length. The cross section area of one augmenter is uniform while the other two are divergent with total included angles of 3^0 and 6^0 .The other three augmenters are uniform in cross section and have ratio of inlet area to primary tube exit area of 12.5 but at lengths 9,15 and 20 cm. All augmenters have a bellmouth inlet to minimize spill over. The pulse frequency of the primary flow is varied by changing the pulse generator speed via the variable speed motor.

Dry, high pressure air is supplied to the rig by screw compressor rated at 8.2 m^3/min. and 10 bars. One primary tube of 8 mm inside diameter and 45 cm length is used. A calibrated thrust meter of the free displacement type is used for thrust measurement of primary and augmenter tube exits.

Theoretical Model

The calculation of the fluid properties in the primary and augmenter flow fields is carried out by the method of characteristics, based on the following partial differential equations representing mass, momentum and energy conservation in one dimension space and in vector notation:

$$\frac{\partial}{\partial t}\begin{Bmatrix}\rho\\ \rho u\\ \rho\left(e+\frac{u^2}{2}\right)\end{Bmatrix}+\frac{\partial}{\partial x}\begin{Bmatrix}\rho u\\ \rho u^2+p\\ \rho u\left(e+\frac{u^2}{2}+\frac{p}{\rho}\right)\end{Bmatrix}=\begin{Bmatrix}-\frac{\rho u}{Ar}\frac{dAr}{dx}\\ -\rho G-\frac{\rho u^2}{Ar}\frac{dAr}{dx}\\ \rho q-\frac{1}{Ar}\left\{\rho u\left(e+\frac{p}{\rho}+\frac{u^2}{2}\right)\right\}\frac{dAr}{dx}\end{Bmatrix} \quad (1)$$

where

$$G=\frac{u}{2}\frac{|u|}{}*\frac{4f}{d} \quad (2)$$

represents the friction force per unit mass with friction coefficient f assumed to be that of quasi-steady turbulent flow [13]. The term q represents the heat transfer per unit mass per unit time:

$$q=\frac{4h_f}{\rho D}(T_w-T) \quad (3)$$

h_f is the film heat transfer coefficient calculated from Reynolds-Colburn analogy [13] and T_w is the wall temperature. Manipulation of the above system of Equations 1, it is transformed into its characteristic form [12,14]. Non dimensionalization of the equations and using the dependent variables, P, U and σ, the ordinary differential equations are integrated along their relevant characteristics [12,14]:

$$\frac{1}{2}(\sigma_B+\sigma_N)P_B+U_B=\frac{1}{2}(\sigma_B+\sigma_N)P_N+U_u+\left(\frac{\gamma-1}{\gamma}D''-F''\right)_{NB}\Delta Z-\left(\frac{P\sigma U}{Ar''}\right)_{NB}\frac{dAr''}{dX}\Delta Z \quad (4)$$

Along (U" + A") characteristics, NB on the (X-Z) plane.

$$\frac{1}{2}(\sigma_B+\sigma_M)P_B+U_B=\frac{1}{2}(\sigma_B+\sigma_N)P_N+U_M+\left(\frac{\gamma-1}{\gamma}D''+F''\right)_{MB}\Delta Z-\left(\frac{P\sigma U}{Ar''}\right)_{MB}\frac{dAr''}{dX}\Delta Z \quad (5)$$

Along (U" - A") characteristics, MB on the (X-Z) plane.

$$\sigma_B-\sigma_J=\frac{1}{2}(\sigma_B+\sigma_J)H''_{JB}\Delta Z \quad (6)$$

Along particle path U" characteristic, JB on the (X-Z) plane.

$$D''=\gamma\frac{(\gamma-1)}{2}\frac{(q^*+U''G^*}{A''}$$

$$E''=\frac{\gamma-1}{2\gamma}A''^2$$

$$H''=\left(\frac{\gamma-1}{2}\right)\frac{\sigma}{A''^2}(q^*+U''G^*)$$

$$F''=\frac{\gamma-1}{2}G^*$$

The above equations are solved algebraically to find the values of the dependent variables at the new time level for internal nodes. The double subscripts denote average quantities over the relevant characteristics.

The missing information required to obtain the dependent variables at the boundary node points of the flow fields, are obtained through the boundary conditions by application of the conservation equations of mass and energy in quasi-steady forms [12,14]. The flow information of the primary flow as it enters the augmenter duct is numerically supplied through mass, momentum and energy balance technique at any instant. Full details of the numerical simulation procedure is available [12,14].

The convergence of the numerical solution of the model to a conditions representing cycle operation is demonstrated. More information including the novel features of the model is detailed in [12,14]. The model is shown capable of interpreting the phenomena within the ejector at great accuracy [12] and proved successful to be used for performance evaluation.

RESULTS AND DISCUSSION

The performance of the pulsed ejector depends on many geometric and operational parameters, some of which are related to the primary jet flow configuration. In applications such as pulsed combustors, pulsed converters and many propulsive devices, the characteristics of the primary jet are controlled by factors other than the ejector i.e. the ejector is required to generate the maximum possible augmenting capacity of mass and thrust under predetermined primary flow configurations. So, no attempt has been made to optimize the primary flow. Instead, the primary flow generated by the primary tube prototype ejector, is employed with the intention of determining the configuration of the augmenter tube capable increasing primary mass and thrust under all primary conditions. The ejector performance depends on primary stagnation pressure p_o , primary jet frequency f, augmenter length to inlet diameter ratio (L/D), ratio of augmenter inlet area to primary tube exit area (A_{aug} /A_j), Augmenter divergence angle (Θ) and also the distance between the augmenter and primary tube exit (x/D). The secondary stagnation pressure, which is the flow box pressure, is also a parameter that controls both the primary and secondary flows. However, it was not taken as an optimization parameter since in most practical applications the secondary stagnation pressure is independent from ejector operation.

It should be noted that the distance between augmenter and primary tube exit as a ratio of the augmenter inlet diameter (x/D) has a major effect on the configuration of the primary jet issuing from the primary tube as it travels to augmenter inlet. If this ratio is very large spill over of the primary jet is inevitable and if it is too small, the primary jet is not developed such that it fails to fill the augmenter inlet area, hence the piston like action of the primary jet is lost in the augmenter tube. Such a phenomena can only be described through a mathematical model of more than one spatial dimension. Experiments were thus performed to obtain an optimum (x/D) value so that the full potentials of the one-dimensional piston like action of the primary jet is realized. Nevertheless, at the experimentally obtained x/D ratio, where the primary jet floods the entire augmenter inlet area, the flow in the augmenter tube is essentially one dimension and hence the numerical model is capable of describing the flow events in the augmenter tube with utmost efficiency. Mass Flow Rate Ratio (m_t /m_p). Figure 5 represents the mass flow rate ratio from experimental measurements as a function of x/D at various primary stagnation pressures. Each figure presents the results at specified area ratio (A_{aug}/A_j), frequency and augmenter divergence angle (Θ). The figures exhibit an optimum x/D ratio of 1.25. Increase of x/D shows a negligible decline of mass flow ratio for high x/D ratio up to the value of 6. Thrust augmentation ratio also showed similar behavior. This implies the augmenter bellmouth collects the primary jet even if the primary jet development exceeds the diameter of the augmenter inlet section.

Figures 6 and 7 show samples of the experimentally measured and the corresponding analytical predictions of mass flow rate ratio , as a function of frequency for different primary stagnation pressures. The results correlate favorably and showing a rising characteristics as the frequency increases due to increased momentum of the primary jet and hence the augmenter secondary flow. However, the mass flow ratio of the ejector decreases as the primary flow stagnation pressure increases.

This is attributed to the increased entropy discontinuity with which the primary flow enters the augmenter. The rarefaction waves, then, weaken upon colliding with the contact discontinuity and hence the depression at the augmenter inlet does not increase the secondary flow with the same proportion as the primary flow. The increase of augmenter divergence angle is shown to enhance the secondary flow due to the increased depression at the augmenter inlet which results from the wave interaction with the diffusing area change.

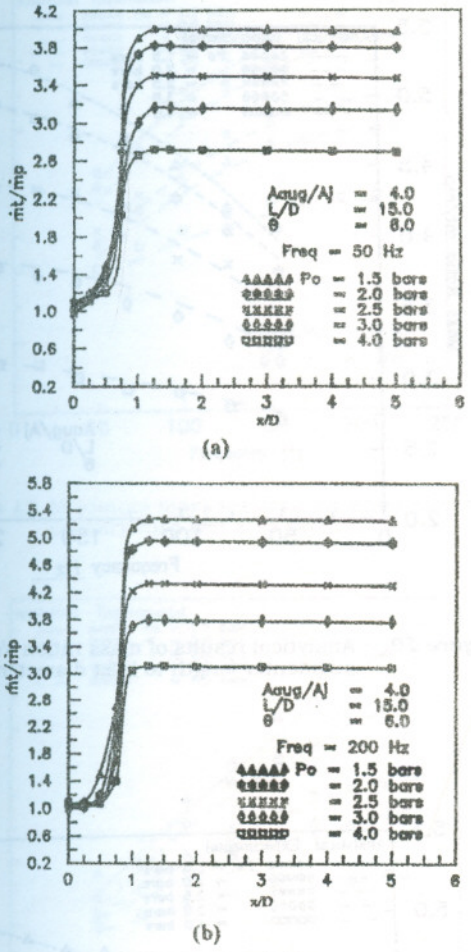

Figure 5 Effect of the distance 'x' between augmenter inlet section and primary tube exit section on the ejector performane (experimental measurement).

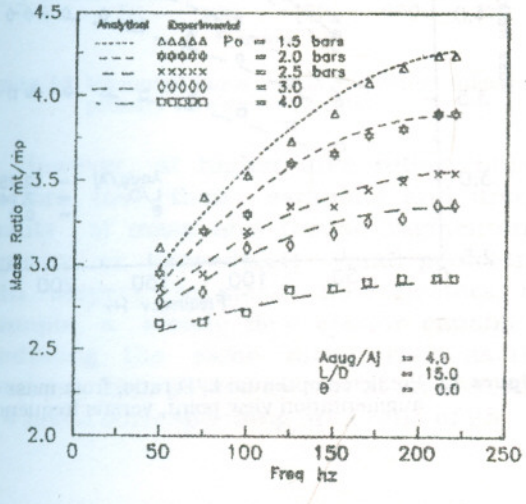

Figure 6 Experimental and analytical results of augmenter tube no. 1

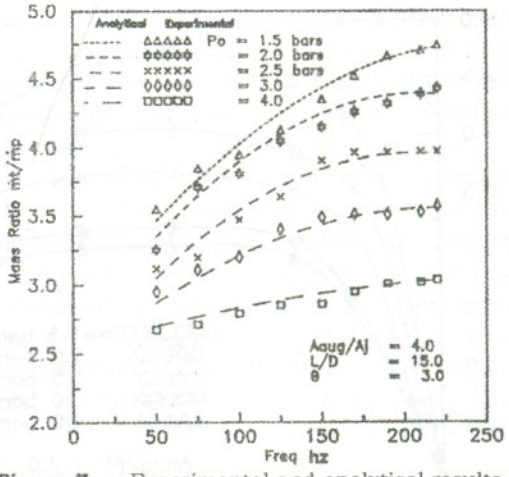

Figure 7 Experimental and analytical results of augmenter tube no. 2

Figures 8 to 10 represent samples of the predicted mass flow ratio as a function of L/D at various stagnation pressures. The optimum L/D ratio is, as shown, a strong function of the area ratio and primary frequency. From each graph, it is clear that the optimum L/D ratio is independent of the primary stagnation pressure and from each two consecutive graphs optimum L/D is also independent of Θ .Figure 11 presents the optimum L/D ratios as a function of frequency at variant area ratio (A_{aug}/A_j). Increasing the primary pulse frequency entails the decrease of the optimum augmenter length, for a certain area ratio, which is required for a tuned ejector that maximizes the wave mechanics effects to draw in more secondary air.

Figures 12 and 13 show a capture of a series of numerical tests of the mass flow ratio as a function of area ratio (A_{aug}/A_j) for a specified divergence angle and frequency at the determined optimum (L/D) ratios. The ever-increasing behavior of mass ratios is attributed to the combined actions of increased primary jet entrainment and augmenter inlet area increase which increases the secondary flow despite the decreased depression at augmenter inlet. The present analysis did not probe the performance beyond area ratio 12 because the flow within the augmenter becomes, then, far from one that can be described by a one dimension model.

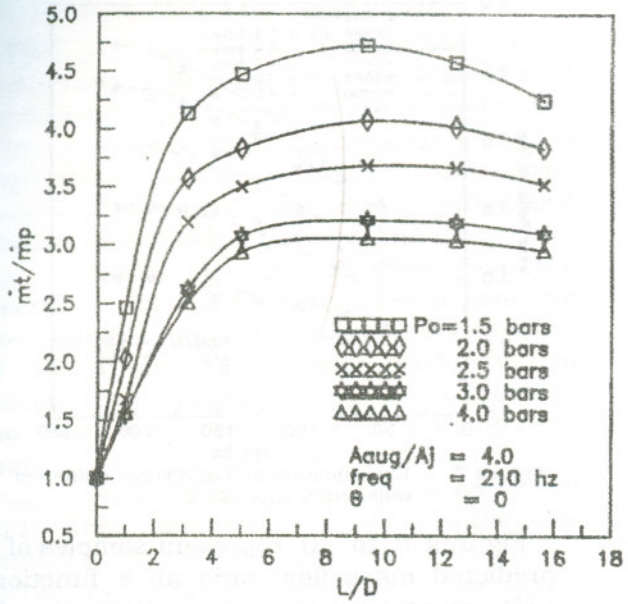

Figure 8 Analytical results of mass ration Vs. augmenter length to inlet diameter ratio

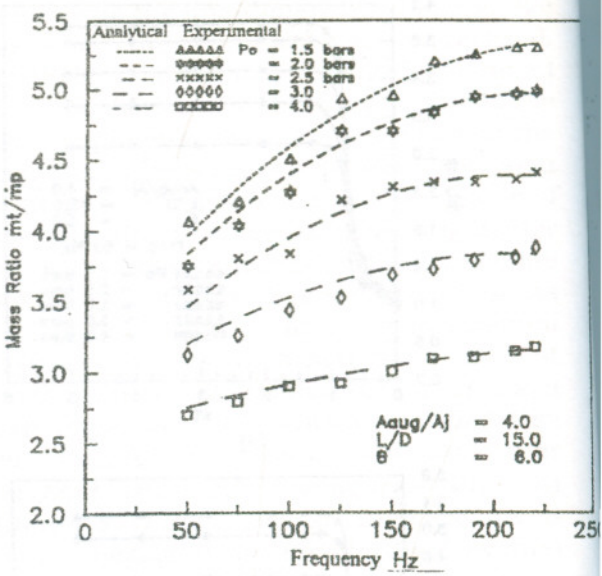

Figure 10 Analytical results of mass ration Vs. augmenter length to inlet diameter ratio.

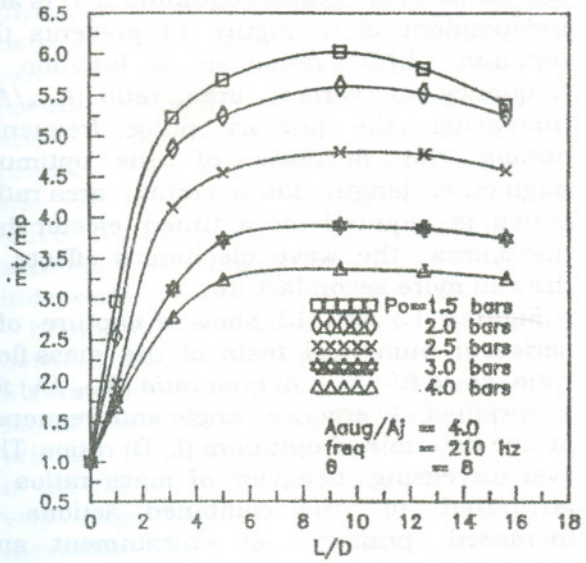

Figure 9 Analytical results of mass ration vs. augmenter length to inlet diameter ratio

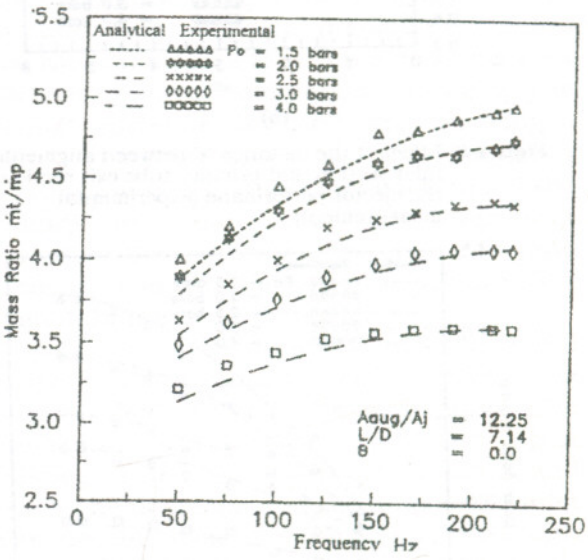

Figure 11 Predicted optimum L/D ratio, from mass augmentation view point, versus frequency.

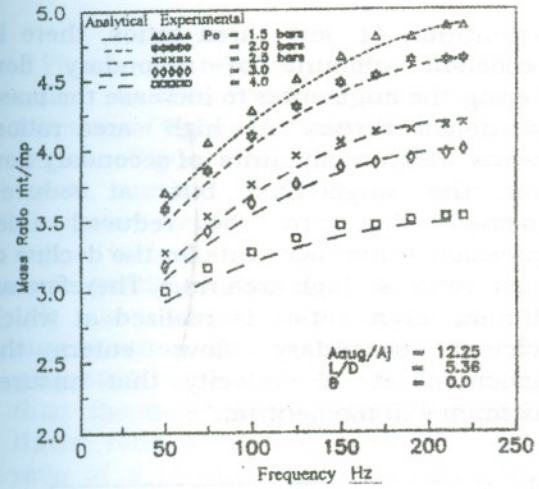

Figure 12 Maximum mass versus augmenter inlet to primary tube exit area ratio.

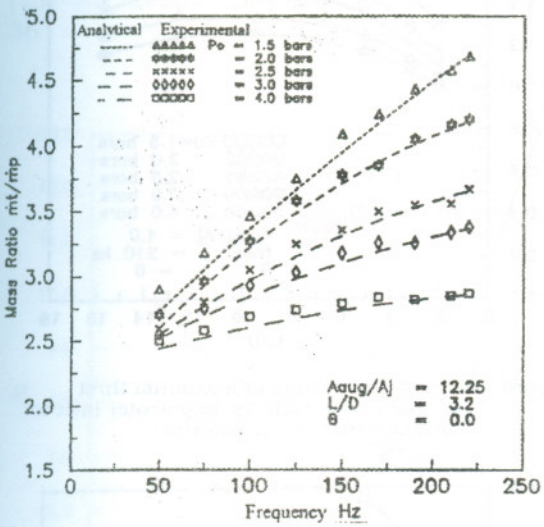

Figure 13 Maximum mass versus augmenter inlet to primary tube exit area ratio.

However, at higher area ratios, pulsed ejectors lose their exquisite and unique quality of mass and thrust augmentation capacity at exceedingly small geometries with respect to steady flow ejectors. For example a steady flow ejector capable of producing the same mass ratio as that obtained from pulsed ejector at an area ratio of 4 has a corresponding area ratio of 25 while using multiple hyper mixing primary nozzles [15]. The figures also show that the mass flow ratio increases as the divergence angle increases. This is due to the increased depression at the augmenter inlet, which increases the inhaled secondary flow.

It is, therefore, concluded from model analysis that, from the point of view of mass augmentation, the area ratio (A_{aug}/A_j) and/or divergence angle increases the ejector performance. Nevertheless, since at higher divergence angles or higher area ratio the performance falls off due to flow separation and the appearance of vortex-flow, which as expected the model then departs from one dimensional flow.

Thrust Augmentation Ratio (T_{aug} /T_p)

The thrust ratio represents the average augmented outlet momentum flux from the augmenter tube divided by that at the primary tube outlet. The average outlet momentum is calculated over one cycle as:

$$T=\frac{\int_0^{\Delta t_{cycle}} \rho A r u^2 dt}{\Delta t_{cycle}}$$

The average thrust force is, calculated accordingly at both the primary and augmenter tube outlets over one cycle after steady cyclic operation is attained. The thrust is measured by the free displacement type thrust meter.

Figures 14 and 15 show samples of series numerical tests representing the thrust ratio (T_{ang} /Tp) as a function of (L/D) at various stagnation pressures. Each figure presents the results at a specified area ratio, frequency and divergence angle. It should be observed that optimum (L/D) is a function of only the area ratio, frequency and divergence angle and is not a function of stagnation pressure.

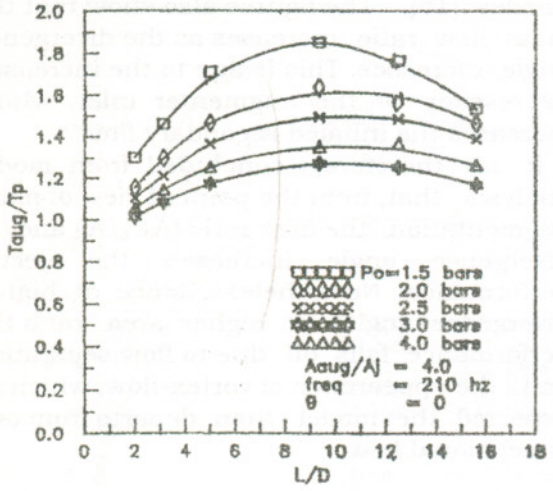

Figure 14 Analytical results of thrust augmentation ration Vs. augmenter length to inlet inlet diameter ratio.

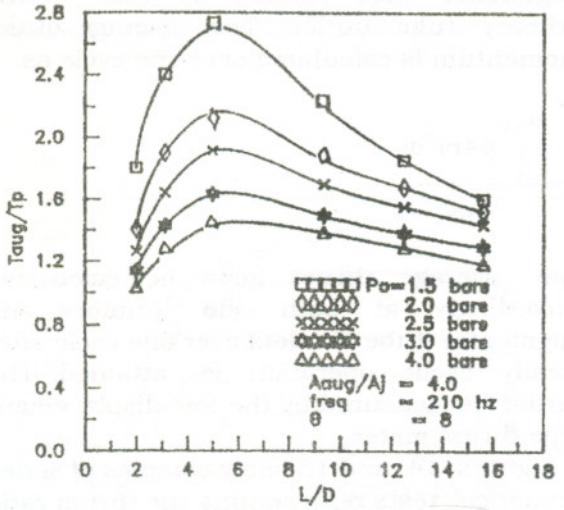

Figure 15 Analytical results of thrust augmentation ration Vs. augmenter length to inlet inlet diameter ratio.

Figures 16 and 17 show the results of the predicted thrust ratio (T_{aug}/T_p) as a function of area ratio (A_{aug}/A_j) at various stagnation pressures and optimum L/D ratio. Each figure represents the results at a specified frequency and divergence angle. It is clear that regardless of frequency, divergence angle and stagnation pressure, an optimum area ratio of 4.15, is obtained. Unlike mass ratio, the thrust augmentation is realized due to increased induced momentum. At low area ratios, there is insufficient amount of secondary flow entering the augmenter to increase the mass and hence thrust. At high area ratios, however, higher amounts of secondary flow enter the augmenter but at reduced velocities due to the reduced inlet depression. This accounts for the decline of thrust ratio at high area ratio. Therefore an optimum area ratio is realized at which sufficient secondary flow enters the augmenter at a velocity that ensures maximum exit momentum.

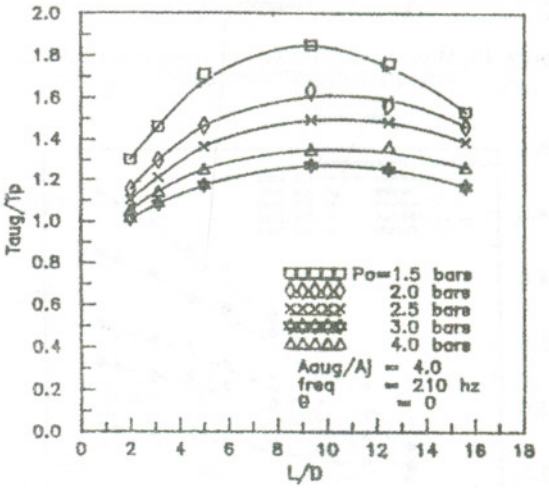

Figure 16 Analytical results of maximum thrst augmentaion ratio vs. augmenter inlet to primary tube exit area ratio.

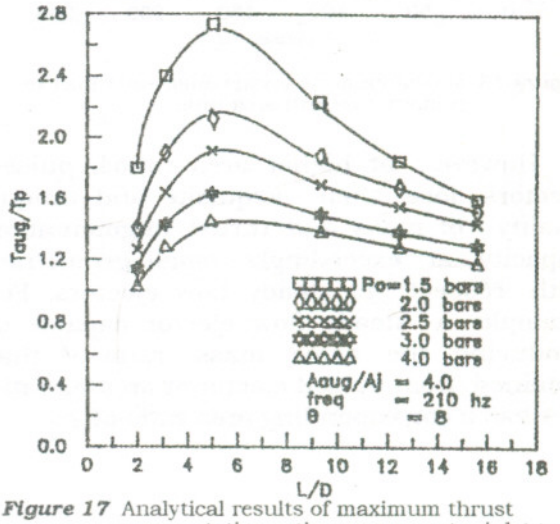

Figure 17 Analytical results of maximum thrust augmentation ratio vs. augmenter inlet to primary tube exit area ratio.

Figure 18 represents the optimum L/D ratios at the optimum area ratio as a function of frequency and various divergence angles. Figure 19 shows the maximum thrust ratio (T_{aug}/T_p) as function of divergence angle at the optimum area ratio and various frequencies and their corresponding optimum L/D ratios.

It is emphasized that the thrust augmentation ratio of the pulsed ejectors are generated at extremely smaller area ratio than the steady flow ejectors. The maximum thrust ratio of 2.45 is realized at an area ratio of 4.15 which compares favorably with the thrust ratio of 2.4 reported by Lockwood [16] for a prototype pulsed ejector at an area ratio of 4. This thrust ratio was reported by [15] for steady flow ejector at an area ratio 36.

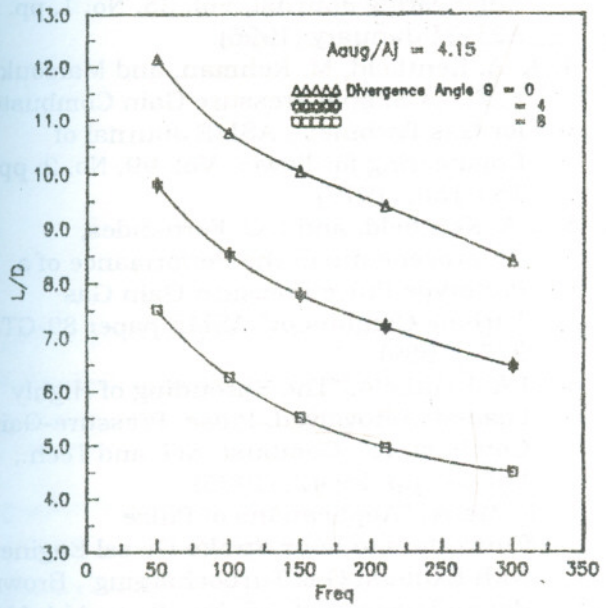

Figure 18 Predicted optimum L/D ratio, from thrust augmentation view point Vs. frequency at optimum area ratio.

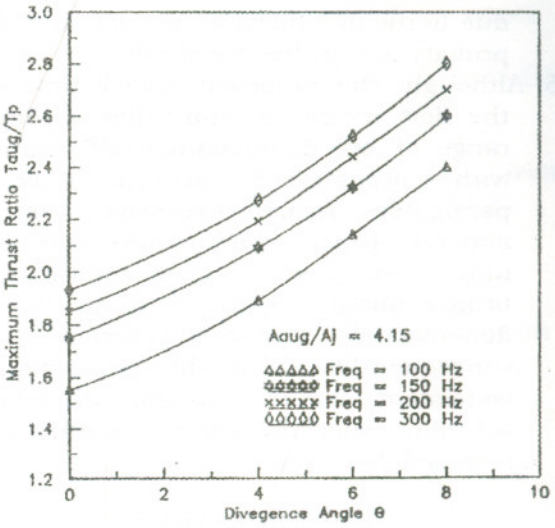

Figure 19 Maximum thrust ratio at optimum area ratio and L/D ratio Vs. divergence angle θ

CONCLUSIONS

From the aforementioned analysis the following is concluded:

1. The pulsed ejector has exceptional capacity to augment the primary mass flow rate and thrust at unusually smaller area ratio (4-4.5) compared to the corresponding steady flow ejectors (25 or more). This capacity depends primarily on the momentum of the primary flow as well as its entropy.
2. The analysis provides the optimum augmenter length to inlet diameter ratios suitable for every specified primary flow configuration generated in devices such as pulsed combustors, pulsed converters and other propulsive devices.
3. The optimum augmenter area ratio is independent from the primary flow configuration. It is, from geometrical view point, an augmenter inlet area capable of capturing the entire primary jet and at the same time maintains strong wave action in the augmenter to increase both mass and momentum to a maximum. The optimum area ratio from point of view of thrust augmentation, is 4.15.
4. The mass augmentation capacity of pulsed ejector continually increases as the area ratio increases due to the inlet duct increased primary flow entertainment and

due to the minimization of spill over of the primary flow at the augmenter.

5. Although the proposed model simulates the flow in the ejector tubes, within the range of one dimensional configurations, with pronounced accuracy, certain parameters, namely excessive area ratio and divergence angle increase, can not be fully investigated because their increase brings about departure from the one dimensional flow behavior and consequently mars the generation of consistent and realistic numerical solution especially when separation and reversed flow occur.

NOMENCLATURE

Symbol	Non dimensional	Meaning
a (m/s)	$A" = a/a_{ref}$	Sonic Speed
Ar (m^2)	$A"r = Ar/Ar_{ref}$	Duct area
D (m)		Augmenter inlet diameter
e (J/kg)		Specific internal energy
G(N/Kg)	$G^* = G\, x_{ref} / a^2_{ref}$	Friction force per unit mass
m(kg/s)	$m=\frac{\gamma m a_{ref}}{p_{ref}.Ar_{ref}}$	Mass flow rate
p (Pa.)	$P"=\frac{p}{p_{ref}}, P = (P")^{\frac{\gamma-1}{2\gamma}}$	Pressure
q (J/kg s)	$q^*=\frac{qx_{ref}}{a^3_{ref}}$	Heat transfer per unit mass
R(J/kg K)		Gas Constant
s(J/Kg K)	$\sigma=e^{\left(\frac{\gamma-1}{\gamma}\right)s/R}$	Entropy
t (sec)	$Z=\frac{ta_{ref}}{x_{ref}}$	Time
T (K), (N)		Static tempe-Rature and thrust
u (m/s)	$U"=u/a_{ref}, U=\frac{\gamma-1}{2}U"$	Gas velocity
x (m)	$X = x / x_{ref}$	Distance

Greak Symbols

γ	Adiabatic index
θ (degree)	Divergence angle
ρ (Kg/m^3)	Gas density

Subscripts

aug	At augmenter tube exit
ref, o	Reference conditions and stagnation conditions
t,p	Total and primary

Superscripts

“ , *	Non dimensional variable

REFERENCES

1. A. A. Putnam, F. E. Belles and J.A. Kentfield “Pulse Combustion”, Progress in Energy and Combustion Science, Vol. 12, No. 1, pp. 43-79 (1986).
2. Proceedings of the Third International Symposium on Pulse Combustion Applications, Alta, Ga, GRI-82/0009.2, NTIS PB82-240060, Vol. 1, (1982).
3. E.M. Marzouk, S.G. and Ahmed, “Gas Dynamic Coupling of Two Valveless Pulsed Combustors for Pressure-Gain Combustion. Chambers”, Alexandria Engineering Journal, Vol. 35, No. 1, pp. A21-31 January (1996).
4. K. A. Kentfield, M. Rehman, and Marzouk, E.M., “A Simple Pressure Gain Combustor for Gas Turbines”, ASME Journal of Engineering for Power, Vol. 99, No. 2, pp. 153-158, (1977).
5. J.A. Kentfield, and L.C. Fernandes, “Improvements to the Performance of a Prototype Pulse Pressure-Gain Gas Turbine Combustor” ASME paper 89-GT-277, (1989).
6. J.A. Kentfield, “The Shrouding of Highly Loaded, Aerovalved, Pulse, Pressure-Gain Combustors”, Combust. Sci. and Tech., Vol. 94, pp. 25-42, (1993).
7. E. Meier, “Applications of Pulse Converters to Four Stroke Diesel Engines with Exhaust Gas Turbocharging”, Brown Boviri Review, Vol. 55, No., 8, pp.414-419, (1968).
8. N.S. Jonata, and N. Watson, “Pulse Converters, A Method of Improving the Performance of Turbocharged Diesel Engine”, Proc. of the Inst. of Mech. Engineers, Vol. 187, No.51/73, pp. 635-647, (1973).
9. D. E. Winterbone, G.I. Alexander and S. K. Sinha “The Evaluation of the

Performance of Exhaust Systems Equipped with Integral Pulse. Converters", Cimac, Int. Congress on Combustion Engines, Oslo, paper D62, (1985).
10. R.M. Lockwood, "Interim Summary Report on Investigation of the Process of Energy Transfer from an Intermittent Jet to a Secondary Fluid in an Ejector Type Thrust Augmente, Report No. ARD-286, Hiller Aircraft Corp. Palo Alto, Ca, (1961).
11. R.M. Lockwood, "Summary Report on Miniature valveless Pulse Jets" Report No. ARD-307, Hiller Aircraft Corp., Palo, Alto, Ca, (1962).
12. E.M. Marzouk, and A. F. Abd Elwahab, "A Numerical Model for Prediction of the Induced Flow in Pulse Jet Ejector with Experimental Verification", AIAA, paper No. AIAA-97-1016, (1997).
13. J. P. Holman, "Heat Transfer", Sixth Ed., McGraw Hill, N.Y., (1986).
14. A. F. Abdel Wahab "Performance and Optimization of Non Steady Pulsed Ejector with Experimental Verification", M.Sc. Thesis, Mech. Eng., Alex. University, (1996).
15. C.C. Kenneth, and A. L. Gerald, "Multiple Hole Ejector Performance with Short Wide Angle Diffusers", J. of Propulsion and Power, AIAA, Vol. 10, No.3, Nay-June (1994).

Received September 30, 1998
Accepted February 6, 1999

تقييم أداء النافث النبضى -نتائج النموذج العددى والنتائج المعملية

السيد محمد مرزوق و أحمد فاروق عبد الوهاب و محمد عواد
و عبد الفتاح ابراهيم عبد الفتاح
قسم هندسة القوى الميكانيكية – جامعة الاسكندرية

ملخص البحث

يستخدم النافث النبضى فى غرف الاحتراق الترددية ذات الضغط المكتسب للتوربينات الغازية أو فى المحولات النبضية تتشاحن التوربينى لمحركات الترددية....إلخ . يحقق البحث فى تاثير بعض العوامل الهندسية وظروف التشغيل على كيفية تصميم وأداء النافث. وقد أستخدم فى البحث نموذج رياضى عددى أحادى البعد للسريان غير المستقر يحاكى كل الظواهر والعمليات التى تحدث داخل النافث النبضى وكذلك القياسات المعملية.

وقد بين البحث قدرة النافث غير العادية على زيادة سريان الكتلة والدفع عند قيم غير عادية فى الصغر لنسبة مساحة مقطع الأنبوب الطارد إلى مساحة مخرج الأنبوب الأبتدائى (4.5-4) بمقارنتها مع نافث السريان المستقر(أكبر من 25).

وقد أدى زيادة الضغط الكلى لهواء السريان الابتدائى الداخل لمولد النبضات, وعلى غير المتوقع, إلى تدنى أداء النافث وذلك نتيجة زيادة الأنتروبيا لنبضة الهواء الابتدائى المرسل للانبوب الدافع وتداخل الموجات التضاغطية وإنعكاساتها مع السطح البينى المتولد مما يقلل من إنخفاض الضغط المتولد عند مدخل الدافع.

كما بين البحث أن النسبة المثلى بين طول وقطر مقطع دخول الانبوب الدافع تعتمد على ذبذبة السريان الإبتدائى. وقد تم الحصول على نسبة مثلى بين مساحة مقطع دخول الانبوب الدافع لمساحة خروج الانبوب الإبتدائى من وجهة نظر السريان الدفعى و ومقدارها 4.5 , إلا أنة لم يمكن الوصول إتى نسبة مثلى من وجهة نظر السريان الكتلى.